

Article

Effect of Coal Particle Breakage on Gas Desorption Rate during Coal and Gas Outburst

Qiang Cheng ^{1,2} , Gun Huang ^{1,2,*}, Zhiqiang Li ³, Jie Zheng ⁴  and Qinming Liang ^{1,2}

¹ State Key Laboratory of Coal Mine Disaster Dynamics and Control, Chongqing University, Chongqing 400030, China; qiangcheng@cqu.edu.cn (Q.C.); qmliang@cqu.edu.cn (Q.L.)

² School of Resources and Safety Engineering, Chongqing University, Chongqing 400030, China

³ Collaborative Innovation Center of Coal Work Safety and Clean High Efficiency Utilization, Henan Polytechnic University, Jiaozuo 454000, China; lizhiqiang@hpu.edu.cn

⁴ School of Geology and Mining Engineering, Xinjiang University, Urumqi 830046, China; jieuan@163.com

* Correspondence: hg023@cqu.edu.cn

Abstract: The gas contained in coal plays a crucial role in triggering coal and gas outbursts. During an outburst, a large quantity of gas originally absorbed by coal is released from pulverized coal. The role this part of the gas plays in the process of coal and gas outbursts has not been clearly elucidated yet. Therefore, investigating the changes in gas desorption rate from coal particles of different sizes could provide some meaningful insights into the outburst process and improve our understanding of the outburst mechanism. First, combining the diffusivity of coal of different particle sizes and the distribution function of broken coal, we present a gas desorption model for fragmented gas-bearing coal that can quantify gas desorption from coal particles within a certain range of size. Second, the gas desorption rate ratio is defined as the ratio of the gas desorption rate from coal being crushed to that from coal before breaking. The desorption rate ratio is mainly determined by the desorption index (γ) and the granularity distribution index (α). Within the limit range of coal particle sizes, the ratio of effective diffusion coefficient for coal particles with different sizes is directly proportional to the reciprocal of the ratio of particle sizes. Under uniform particle size conditions before and after fragmentation, the gas desorption rate ratio is the square root of the reciprocal of the effective diffusion coefficient. The gas desorption model quantitatively elucidates the accelerated desorption of adsorbed gas in coal during the continuous fragmentation process of coal during an outburst.



Citation: Cheng, Q.; Huang, G.; Li, Z.; Zheng, J.; Liang, Q. Effect of Coal Particle Breakage on Gas Desorption Rate during Coal and Gas Outburst. *Appl. Sci.* **2024**, *14*, 469. <https://doi.org/10.3390/app14010469>

Academic Editor: Fulvia Chiampo

Received: 1 December 2023

Revised: 27 December 2023

Accepted: 31 December 2023

Published: 4 January 2024



Copyright: © 2024 by the authors. Licensee MDPI, Basel, Switzerland. This article is an open access article distributed under the terms and conditions of the Creative Commons Attribution (CC BY) license (<https://creativecommons.org/licenses/by/4.0/>).

Keywords: coal and gas outbursts; pulverized coal; gas desorption rate; effective diffusion coefficient; particle size distribution

1. Introduction

Coal is a significant energy source worldwide, but coal mining presents considerable safety and environmental hazards, including coal and gas outbursts that pose a significant risk of fatality and property damage [1,2]. An instantaneous coal outburst is an abrupt and violent ejection of coal and gas during underground mining [3,4], characterized by the sudden emission of a large quantity of gas accompanying pulverized coal into the underground roadways in a short period of time [1,2]. Despite the recognized correlation between coal gas outbursts and factors such as gas contents in coal, geological conditions, and ground stress, the underlying mechanisms responsible for outbursts are not yet fully comprehended [5–7]. With the increase in burial depth, the outburst intensity increases remarkably. This is mainly due to changes in geological structure and coal seam thickness, which affect gas pressure and ground stress. As a result, the failure mode changes from tensile to shear failure, with higher unloading rates making tensile failure more likely. Additionally, under a higher gas desorption rate, the scope of the non-failure zone becomes smaller [8].

Coal is an adsorbent material with complex structures. More than 90% of methane gas is absorbed into the coal matrix; the rest is free gas existing in the pores of the coal. The impact of volatiles on the porous structure of coal samples and the resulting changes in methane adsorption capacity [9]. Volatile-related deformations in the coal's porous structure influenced methane adsorption behavior. Microstructural characterizations revealed that volatiles could be found trapped in the pores or cross-linked in the network, with each state affecting different aspects of coal-coal interactions and the overall structure of coal. Coal consists of fracture networks and coal matrix blocks that are interlocked and distributed without overlapping relationships [10,11]. Matrix blocks in coal contain numerous pores that serve as storage sites for gas and facilitate its flow. Gas is primarily extracted through fractures and pore channels within the coal [12]. The emission of gas from coal is often associated with three phenomena: specific **desorption** from the coal surface, **gas diffusion** within the grains, and gas filtration through a system of fractures in the coal bed [13,14].

Outburst-prone coal is characterized by low mechanical strength and easily crumbles into tiny particles, typically below 1 mm in size. Coal breakage will not only result in changes in particle size distribution but also accelerate gas desorption from coal to release a huge amount of gas, which may participate directly or indirectly in the outburst process [15,16]. The effect of coal size needs to be considered in the outburst process [17]. Therefore, deep insights into coal and gas outbursts require analyzing gas desorption rate variations in gas-containing coal pre- and post-crushing. It has already been recognized in addressing the outburst issue that the desorption rate of gas from coal is closely associated with the tendency of coal outbursts [18,19]. The rapid gas desorption from powdered coal plays a decisive role in gas outbursts [20,21]. Furthermore, the gas release during the initial stage is closely linked to the level of outburst risk [22]. As a result, certain coal-producing countries developed a standard procedure for an index known as the initial gas emission velocity, which involves measuring the amount of gas released over time from coal cuttings collected from soft coal layers within coalbeds [23]. Therefore, analyzing the relationship between coal breakage and gas desorption rate can aid in understanding the significant gas release that occurs during the outburst process.

The main factors affecting gas desorption rate involve gas adsorption equilibrium pressure and coal particle size. The desorption amount increases with higher equilibrium pressure and smaller coal particles [24]. Airey and Bertard et al. discovered through their studies that the diffusivity of coal particles is minimally affected by increasing particle size beyond a certain threshold (~6 mm) [15,25]. Similarly, Yang and Wang demonstrated experimentally that a size limit exists for the rate of gas emission from coal particles [26]. Within the limit, the gas discharging rate decreases as the particle size increases, a phenomenon that is not apparent when the coal particle size exceeds the size limit. To investigate this, the gas diffusion amount was measured at different times for gas-bearing coal particles classified according to their size using sieving techniques. Busch et al. claimed that gas transport along cracks or cleats becomes the critical factor while the inter-cleat diffusion distances remain basically constant in larger particles [27]. Conditions being equal, the finer the coal sample, the greater the initial release rate [19]. Once the coal particle size is reduced, rapid gas desorption can then take place [5]. Yao et al. indicated in their work that the size effect of the gas desorbing rate from coal particles is due to the fact that the smaller the constituent coal grains, the shorter the route for absorbed gas to escape from inside the coal, which accordingly implies a faster gas desorbing rate and a severer outburst proneness [28].

Interpreting desorption rate experiments requires a combined gas desorption model on the coal particle scale. Generally, gas desorption amount from coal follows the rule of the square root of desorption time, which is derived from the unipore diffusion model [29–32]. The unipore diffusion model accurately describes gas diffusing behavior in porous media with a unipore structure. However, it fails to produce an accurate fit for gas diffusion in coal due to the complexity of the coal structure. As a result, several models have been proposed by assuming a dual porosity structure [33–35]. Subsequently, diffusion models have been

developed to more accurately represent gas transport in coal by further prioritizing pore structure assumptions in coal [23,36]. In diffusion models, the observed temporal decrease in the diffusion coefficient is addressed through a proposed time-dependent model derived using variable separation [37,38]. The multi-scale dynamic diffusion model introduces the decay coefficient as a key parameter to describe gas diffusion decay in coal. This concept is extended to larger-scale coal cores, encompassing the entire gas diffusion process [39,40]. Additionally, a microscopic analysis is conducted to examine the multi-scale dynamic diffusion mechanism of gas in coal [41]. Sophisticated gas diffusion models will help researchers calculate the gas diffusing rate accurately in coal particles of different sizes [42].

At the same time, the experimental studies show that the effective diffusion coefficient and gas desorption rate increase as the particle size decreases [19,26,43,44]. Zhang et al. quantitatively studied the gas desorption rate based on the gas emission model [19]. Zhao et al. derived that the average desorption speed of gas-bearing coal is inversely proportional to particle size by assuming a constant diffusion coefficient [45]. Despite significant research efforts, there is still a lack of theoretical understanding regarding the relationship between effective diffusion coefficients and coal grain size based on diffusion models.

The crushed coal particles in the outburst process have different particle distributions. The most commonly used models for particle size distribution currently include the Gates-Gaudin-Schuhmann (GGS) model, the Rosin-Rammler (RR) model, the Lognormal model, the Normal model, et al. [46,47]. The smaller the coal particles are crushed, the greater the increase in desorption rate. However, previous studies disregard the analysis of how the distribution of coal particle fragmentation affects the desorption rate. Therefore, this knowledge gap poses a challenge in establishing models that can accurately predict changes in gas desorption rates after coal crushing. More in-depth investigations are necessary to analyze the gas desorption rate in coal with different particle sizes.

The purpose of this study was to develop a gas desorption model for fragmented gas-bearing coal that considers particle size distribution. By calculating the change in gas desorption rate before and after coal fragmentation, this study explained the rapid release of desorption gas during the outburst process. These findings provided valuable insights into the underlying mechanisms of this phenomenon.

2. Model

2.1. Desorption Model for Breakage Gas Bearing Coal

For simplicity, if coal is assumed to be homogeneous and spherical in shape and its diffusion coefficient is constant, then its diffusion model with boundary conditions being constants is [31]:

$$\begin{cases} \frac{\partial C}{\partial t} = D \left(\frac{\partial^2 C}{\partial r^2} + \frac{2}{r} \frac{\partial C}{\partial r} \right) & (0 < r < R_0, t > 0) \\ \frac{\partial C}{\partial r} \Big|_{r=0} = 0, C|_{r=R_0} = C_a & (t > 0) \\ C|_{t=0} = C_0 & (r \geq 0) \end{cases} \quad (1)$$

where C is the gas concentration within coal, g/cm^3 ; C_a is the gas concentration at the boundary, g/cm^3 ; C_0 is the initial gas concentration in the coal particle, g/cm^3 ; D is the gas diffusion coefficient for coal particles, cm^2/s ; $D_e = D/R_0^2$ is the gas effective diffusion coefficient for coal particles, $1/\text{s}$; t denotes time, s ; R_0 is the radius of coal particles, cm .

Solving Equation (1) leads to the ratio of the accumulative gas diffusion quantity to the limiting accumulative diffusion quantity from the coal particle, so-called gas diffusivity for a coal particle.

$$\frac{M_t}{M_\infty} = g(D_e(R_0), t) \quad (2)$$

where M_∞ is the corresponding quantity after infinite time for a certain mass of coal; M_t is the accumulative amount of gas desorbing after time t . Equation (2) proves that the gas

diffusivity is determined by the effective gas diffusion coefficient $D_e(R_0) = D/R_0^2$. When the effective gas diffusion coefficient stays constant, the gas diffusivity increases over time.

Several models, including the Gaudin-Schumann distribution, the Rosin-Rammler distribution, the Gaussian distribution, and the Fractal distribution, have been proposed to describe the particle distribution of broken coal [46,47]. The size of constituent coal grains ranges between $[R_{\min}, R_{\max}]$, where R_{\min} and R_{\max} are a definite number.

Then, the volume of coal grains with a size of R occurs can be written as:

$$dV(R) = \varphi(R)V_0dR \quad (3)$$

where V_0 is the total coal volume; $\varphi(R)$ is the function of grain size distribution; Then, the size distribution function for sieved coal volume could be expressed as $\int_0^R \varphi(R)dR$.

The ultimate gas amount released from a certain mass of coal sample is constant and unchangeable if given long enough time to desorb. Then, the total amount of gas desorption after infinite time can be calculated as follows:

$$M_\infty = (C_0 - C_a)V_0 \quad (4)$$

Meanwhile, the ultimate gas desorption amount remains constant and unaffected by coal particle size distribution. This is because most of the gas in coal is adsorbed onto the micropores of the coal matrix, which are not influenced by changes in particle size that mainly impact mesopore characteristics [48,49].

Further, if we assume the gas diffusivity for coal grains with a size of R is $g(D_e(R), t)$, we can derive the gas desorption volume M_t as

$$M_t = M_\infty \int_{R_{\min}}^{R_{\max}} g(D_e(R), t)\varphi(R)dR \quad (5)$$

Then, gas diffusivity for broken coal is:

$$g(D_e(R), t) = \int_{R_{\min}}^{R_{\max}} g(D_e(R), t)\varphi(R)dR \quad (6)$$

2.2. Desorption Rate Ratio

Here, we define the gas desorption rate as the first-order derivative of the gas desorption volume with respect to time M_t , so the gas desorption rate can be described by:

$$M'_t = M_\infty \int_{R_{\min}}^{R_{\max}} g'(D_e(R), t)\varphi(R)dR \quad (7)$$

Equations (5) and (7) show that both the desorption amount and rate are mainly determined by the adsorption amount, effective diffusion coefficient, and particle size distribution function.

Combining Equation (5) yields the change in desorption amount before and after coal crushing.

$$\eta(t) = \frac{\int_{R_{\min}}^{R_{\max}} g(D_e(R), t)\varphi(R)dR}{\int_{R_{\min}}^{R_{\max}} g(D_e(R), t)\psi(R)dR} \quad (8)$$

which represent the difference in the gas desorption volume during a time interval t before and after coal fragmentation. Where $\psi(R)$ is the function of coal grain size distribution before coal breakage; $\varphi(R)$ represents the function of coal grain size distribution after coal breakage. Equation (8) specifies that this change in the gas desorption volume over time is correlated with the gas diffusivity for coal grains and the distribution function of coal grains.

The concept of gas desorption rate ratio was introduced to characterize the changes in the gas desorption rate of coal before and after crushing. Combining Equation (7) yields the change in the instantaneous gas desorption rate before and after coal.

$$\zeta(t) = \frac{\int_{R_{\min}}^{R_{\max}} g'(D_e(R), t) \varphi(R) dR}{\int_{R_{\min}}^{R_{\max}} g'(D_e(R), t) \psi(R) dR} \tag{9}$$

Equation (9) indicates that the variation of the gas desorption rate ratio is determined chiefly by the gas diffusivity of coal grains and the coal particle size distribution.

2.2.1. Relationship between Effective Diffusion Coefficient and Particle Size

The diffusivity obtained from the solution of the diffusion Equation by the method of separate variables and the method of Laplace transformation are, respectively. The unipore diffusion model is:

$$g(D_e(R_0), t) = 1 - \frac{6}{\pi^2} \sum_{n=1}^{\infty} \frac{1}{n^2} \exp(-n^2 \pi^2 D_e t) \tag{10}$$

$$g(D_e, t) = \frac{M_t}{M_{\infty}} = 6 \cdot \sqrt{D_e t} \left(\frac{1}{\sqrt{\pi}} + 2 \sum_{n=1}^{\infty} \text{ierfc} \frac{n}{\sqrt{D_e t}} \right) - 3 D_e t \tag{11}$$

The effective diffusion coefficient in the dynamic diffusion coefficient model is expressed as:

$$D_e = D_{e0} e^{-\beta t} \tag{12}$$

where D_{e0} is the initial effective diffusion coefficient for gas diffusion in coal; β is the decay coefficient.

The specific form of diffusivity is obtained by solving the diffusion Equation using the separated variable method and the Laplace transform method when the diffusion coefficient varies with time. The dynamic diffusion model is:

$$g(D_{e0}(R), \beta(R), t) = \frac{M_t}{M_{\infty}} = 1 - \frac{6}{\pi^2} \sum_{n=1}^{\infty} \frac{1}{n^2} \exp\left(-n^2 \pi^2 \frac{D_{e0}(1 - e^{-\beta t})}{\beta}\right) \tag{13}$$

$$g(D_{e0}(R), \beta(R), t) = \frac{M_t}{M_{\infty}} = 6 \cdot \sqrt{\frac{D_{e0}(1 - e^{-\beta t})}{\beta}} \left(\frac{1}{\sqrt{\pi}} + 2 \sum_{n=1}^{\infty} \text{ierfc} \frac{n}{\sqrt{\frac{D_{e0}(1 - e^{-\beta t})}{\beta}}} \right) - 3 \frac{D_{e0}(1 - e^{-\beta t})}{\beta} \tag{14}$$

In a specific case, the coal particles are of the same size before and after breakage, with coal being broken down into particles of a single size corresponding to a specific distribution. Taking the most simplified case as an example, the radius of coal particles before breaking is R_1 and after crushing is R_2 . The coal particle size distribution function before and after coal is broken can be expressed as:

$$\begin{aligned} \psi(R) &= \delta(R - R_1) = \begin{cases} 0 & (R \neq R_1) \\ \infty & (R = R_1) \end{cases} \\ \varphi(R) &= \delta(R - R_2) = \begin{cases} 0 & (R \neq R_2) \\ \infty & (R = R_2) \end{cases} \end{aligned} \tag{15}$$

The substitution of Equations (10) and (15) into Equation (8) leads to the variation of the accumulative gas diffusion before and after coal is broken.

$$\eta(t) = \frac{g(D_e(R_2), t)}{g(D_e(R_1), t)} = \frac{1 - \frac{6}{\pi^2} \sum_{n=1}^{\infty} \frac{1}{n^2} \exp(-n^2 \pi^2 D_e(R_2) t)}{1 - \frac{6}{\pi^2} \sum_{n=1}^{\infty} \frac{1}{n^2} \exp(-n^2 \pi^2 D_e(R_1) t)} \tag{16}$$

Substituting Equations (10) and (15) into Equation (9) produces changes in the desorbing rate before and after coal breakage as:

$$\zeta(t) = \frac{g'(D_e(R_2), t)}{g'(D_e(R_1), t)} = \frac{D_e(R_2) \sum_{n=1}^{\infty} \exp(-n^2 \pi^2 D_e(R_2) t)}{D_e(R_1) \sum_{n=1}^{\infty} \exp(-n^2 \pi^2 D_e(R_1) t)} \quad (17)$$

which is the radius of coal with two sizes, R_1, R_2 respectively. M'_{t1} and M'_{t2} represent the gas desorption rates of coal at different times before and after coal crushing, respectively, per unit mass of coal.

The gas desorption rate ratio of the two coal sizes at the initial time, i.e., $t = 0$, is

$$\zeta(0) = \frac{g'(D_e(R_2), 0)}{g'(D_e(R_1), 0)} = \frac{D_e(R_2)}{D_e(R_1)} \quad (18)$$

Equation (18) illustrates that the change in the gas desorbing rate before and after coal breakage can be expressed as the ratio of the effective gas diffusion coefficient.

Methane flows through multiscale pores via a stepwise mechanism from interior to surface pores. Once desorption of gas is possible under favorable conditions, gas molecules near the surface of coal particles start escaping into the surroundings first. Therefore, the cumulative amount of gas desorbed from coal during the initial short period is mainly determined by the surface area of coal particles, which is approximately equal to the gas desorption rate if the period is sufficiently short. Since the volume of coal is constant after being broken, the change in total surface areas would be characterized by differences in the specific surface area of coal particles corresponding to intact coal and broken coal, respectively. The specific surface area of a smaller particle is greater than that of a larger particle. Therefore, we assumed that the initial gas diffusion rate was proportional to the apparent surface area of coal particles. Therefore, we assume the relationship between the size ratio and the initial diffusion rate ratio is

$$\frac{D_e(R_2)}{D_e(R_1)} = \left(\frac{d_1}{d_2}\right)^\gamma = \left(\frac{R_1}{R_2}\right)^\gamma \quad (19)$$

where γ is the index of desorption; d_1, d_2 are the intact and broken coal particle sizes, respectively; The parameter γ represents the change in the effective diffusion coefficient with particle size. The larger γ is, the greater the change in the effective diffusion coefficient after coal crushing. When the coal particle is not broken, the gas desorption rate ratio and specific surface area ratio are equal at the initial time.

Then, the relationship between the effective diffusion coefficients of coal with different particle sizes is:

$$D_{e0}(R) = D_{e0}(R_0) \left(\frac{R_0}{R}\right)^\gamma \quad (20)$$

2.2.2. Approximation of the Desorption Rate Ratio

The distribution pattern of pulverized coal particles can be analyzed using the Gates-Gaudin-Schuhmann (GGS) model, which is expressed as:

$$F = \left(\frac{d}{d_{\max}}\right)^\alpha \quad (21)$$

where F is the volume percentage of particles with a diameter smaller than d ; d is the particle diameter; d_{\max} is the maximum particle diameter; α is the distribution index of granularity, which means the degree of coal particle fragmentation.

Equation (21) can also be written as:

$$F(R) = \left(\frac{R}{R_{\max}} \right)^\alpha \tag{22}$$

The derivative of Equation (22) with respect to particle size yields the particle size distribution, which is given by:

$$\varphi(R) = \alpha \frac{R^{\alpha-1}}{R_{\max}^\alpha} \tag{23}$$

By Equations (9) and (14), the gas desorption rate ratio of coal before and after crushing can be approximately obtained in a short period of time as follows:

$$\zeta(t) = \frac{\int_{R_{\min}}^{R_{\max}} \sqrt{\frac{D_{e0}(R)}{\pi}} \sqrt{\frac{\beta(R)}{1-e^{-\beta(R)t}}} e^{-\beta(R)t} \varphi(R) dR}{\int_{R_{\min}}^{R_{\max}} \sqrt{\frac{D_{e0}(R)}{\pi}} \sqrt{\frac{\beta(R)}{1-e^{-\beta(R)t}}} e^{-\beta(R)t} \psi(R) dR} \tag{24}$$

Assuming that coal exists in a fixed particle size composition before crushing, which changes into different particle sizes after crushing, the particle size distribution of coal before fragmentation and crushing can be expressed as:

$$\psi(R) = \delta(R - R_{\max}) \tag{25}$$

which R_{\max} is the radius of particles before coal breakage. The upper limit of the integral in Equation (24) is also R_{\max} . Substituting Equations (23) and (25) into (24) yields that the desorption rate ratio is:

$$\begin{aligned} \zeta(t) &= \frac{\int_{R_{\min}}^{R_{\max}} 3 \cdot \sqrt{\frac{D_{e0}(R)}{\pi}} \sqrt{\frac{\beta(R)}{1-e^{-\beta(R)t}}} e^{-\beta(R)t} \alpha \frac{R^{\alpha-1}}{R_{\max}^\alpha} dR}{\int_{R_{\min}}^{R_{\max}} 3 \cdot \sqrt{\frac{D_{e0}(R)}{\pi}} \sqrt{\frac{\beta(R)}{1-e^{-\beta(R)t}}} e^{-\beta(R)t} \delta(R - R_{\max}) dR} \\ &= \frac{\int_{R_{\min}}^{R_{\max}} \sqrt{\left(\frac{R_{\max}}{R}\right)^b} \sqrt{\frac{\beta(R)}{1-e^{-\beta(R)t}}} e^{-\beta(R)t} \alpha \frac{R^{\alpha-1}}{R_{\max}^\alpha} dR}{\sqrt{\frac{\beta(R_{\max})}{1-e^{-\beta(R_{\max})t}}} e^{-\beta(R_{\max})t}} \end{aligned} \tag{26}$$

When the decay coefficient β changes little with the decrease in particle size, Equation (26) can be simplified as

$$\begin{aligned} \zeta(t) &\approx \int_{R_{\min}}^{R_{\max}} \sqrt{\frac{D_{e0}(R)}{D_{e0}(R_{\max})}} \alpha \frac{R^{\alpha-1}}{R_{\max}^\alpha} dR \\ &= \int_{R_{\min}}^{R_{\max}} \sqrt{\left(\frac{R_{\max}}{R}\right)^\gamma} \alpha \frac{R^{\alpha-1}}{R_{\max}^\alpha} dR \\ &= \begin{cases} \alpha \ln \frac{R_{\max}}{R_{\min}} & \alpha = \gamma/2 \\ \frac{\alpha}{\alpha-\gamma/2} \left(1 - \left(\frac{R_{\min}}{R_{\max}}\right)^{\alpha-\gamma/2}\right) & \alpha \neq \gamma/2 \end{cases} \end{aligned} \tag{27}$$

Equation (27) demonstrates that the change in gas desorption rate before and after coal crushing can be determined by applying the rules of particle crushing distribution and effective diffusion coefficient.

3. Experiment

The experiment requires measuring the desorption of coal with varying particle sizes at equilibrium adsorption pressure and determining the particle size distribution of crushed coal. As previous studies have extensively researched the desorption experiments of coal with different particle sizes, this paper analyzes the desorption patterns of coal with various particle sizes utilizing existing research data [13,26,43,50–52]. Yang conducted diffusion experiments on anthracite coal with different particle sizes from the No. 1 Mine in Yangquan, Shanxi [26]. Guo conducted similar experiments using anthracite coal samples

from the No. 7 coal seam of the Haizi Coal Mine in the Huaibei Coalfield, China [43]. Wang used coking coal from No. 10 Mines in Pingdingshan, Henan.

During the outburst process, the coal particles are broken due to collisions with each other. In experiments, the date of Cai was selected for verification, and the coal sample with a particle size of 1–2 mm and a mass of 50 g was ground and crushed using a ball mill at 150 r/min and 250 r/min. The crushing tests used samples of bituminous coal obtained from the Nangtiao Tower Mine in Shenmu, Shanxi, as well as samples of coking coal sourced from the No. 10 Mine in Pingdingshan, Henan [53]. In engineering, the data that the outburst coal samples were sieved after outbursts occurred in Zhongliangshan Coal Mine was selected.

4. Results

4.1. Relationship between Effective Diffusion Coefficient and Particle Size

Yang et al., as well as Guo et al., conducted gas diffusion experiments on coal particles of various sizes collected from Yangquan and Haizi coal mines, respectively [26,43]. The short-time average effective diffusion coefficient is similar to the initial effective diffusion coefficient. Guo obtained the average effective diffusion coefficient of coal with different particle sizes at different times under an adsorption equilibrium pressure of 1 MPa [43]. In the short term, the initial effective diffusion coefficient is approximately equal to the average effective diffusion coefficient. Select a kind of coal, such as intact coal in Pingmei No. 10 coal mine, and analyze the initial effective diffusion coefficient of coal with different particle sizes under different adsorption equilibrium pressure conditions [52]. As shown in Figure 1, the effective diffusion coefficients for coal particles with different particle sizes were fitted using Equation (20).

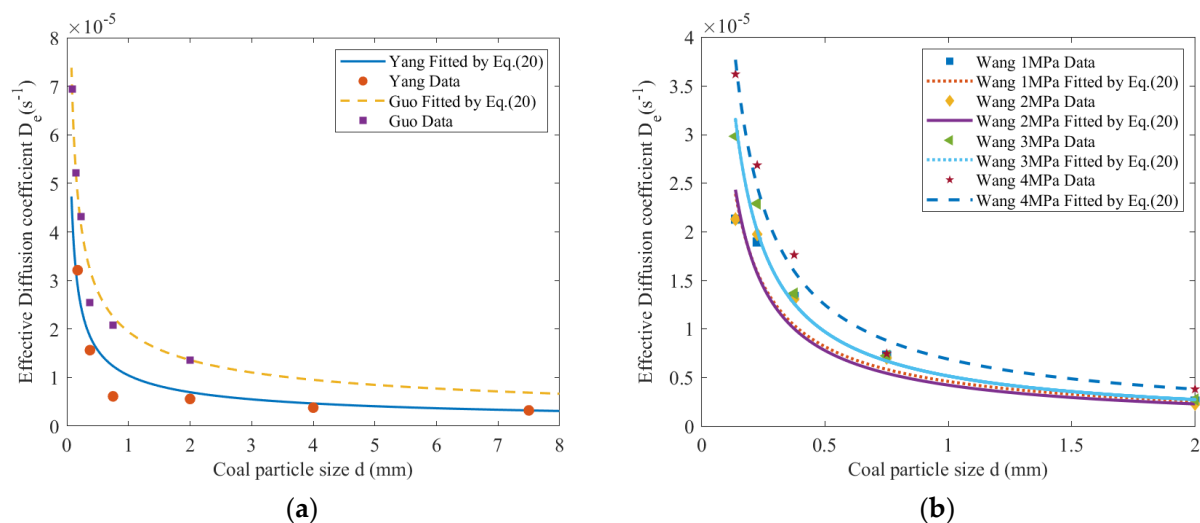


Figure 1. The relationship between effective diffusion coefficient and particle size (a) The data from Yang and Guo; (b) The data from Wang.

Figure 1 demonstrates that the effective diffusion coefficient decreases with increasing particle size for different particle sizes. Use Equation (20) to fit the effective diffusion coefficients of coal with different particle sizes, and the fitting results are shown in Table 1.

Table 1. The fitting results of the effective diffusion coefficients of coal with different particle sizes.

No.	Pressure (MPa)	Index of Desorption γ	Coefficient of Determination
Yang	1	0.5829	0.9303
Guo-1	1	0.5149	0.9822
Wang-1	1	0.8278	0.9221
Wang-2	2	0.8801	0.8996

Table 1. Cont.

No.	Pressure (MPa)	Index of Desorption γ	Coefficient of Determination
Wang-3	3	0.9106	0.9796
Wang-4	4	0.8541	0.9843

4.2. Gas Desorption Rate Ratio of Coal Crushed into Different Single Particle Sizes

The gas-bearing coal diffusivity was obtained by substituting the diffusion coefficient into Equation (2). Using a unipore diffusion model to analyze Yang’s data, the diffusivity of gas-bearing coal with different particle sizes at different times under the same adsorption equilibrium pressure are shown in Figure 2.

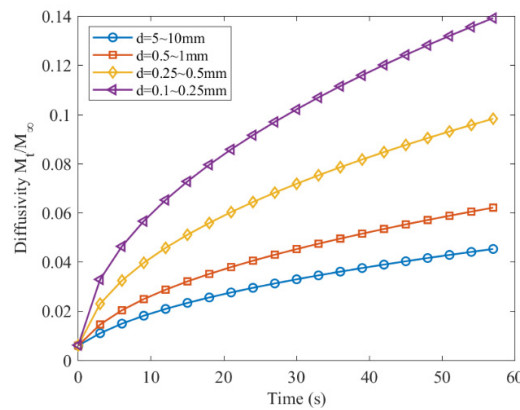


Figure 2. Diffusivity of gas-bearing coal with different particle sizes (Yang).

The degree of coal breakage can be described by the coal particle breakage ratio, defined as $R_1/R_2 = x$, where R_2 is the average particle size after breakage and R_1 is the initial particle size. A higher value corresponds to a greater degree of coal breakage.

By selecting a certain particle size as the reference and substituting it into Equation (16), where the initial coal particle size is 7.5 mm in the data of Yang, the ratio of accumulative desorption amount can be calculated by Equation (16) when coal are crushed into different particle sizes.

Figure 3 depicts the time-dependent ratios of accumulated gas desorption from broken coal particles to that from intact coal particles. These ratios show a rapid increase with time, reaching a peak and then gradually declining to 1. The peak values of these ratios increase with increasing coal breakage ratios (x values), and the rate of increase is higher for larger x values. Additionally, the faster the ratio soars, the steeper the ratio subsequently drops.

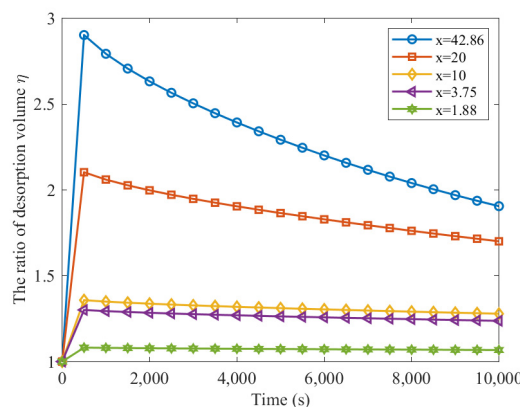


Figure 3. The ratio of desorption volume after and before coal has been broken for a long time.

Using the effective diffusion coefficients in Figure 1 and Equation (16), the desorption amount ratios for the various coal sizes over a short period are presented in Figure 4.

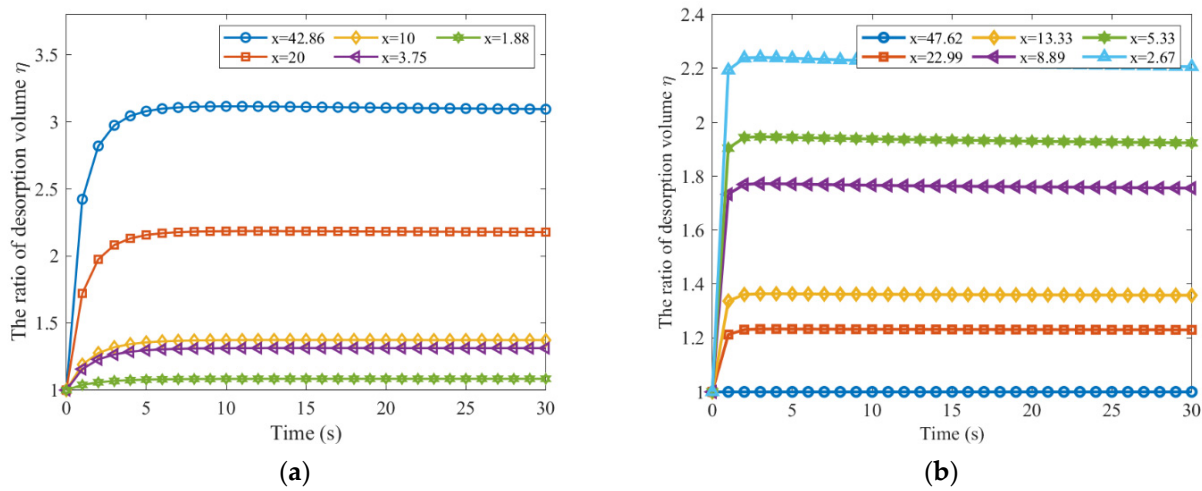


Figure 4. The ratio of gas cumulative diffusion after and before coal is broken in a short time: (a) Effective diffusion coefficient from Yang; (b) Effective diffusion coefficient from Guo.

By integrating the experimental data presented in Figure 1, the ratio of gas desorption rates for coal particles of different sizes after crushing can be calculated using Equation (17) when the initial coal particle size is 7.5 mm. For the data reported by Guo, the maximum particle size were used as the initial particle size to evaluate the change in diffusion rate for a short period before and after coal crushing, and the results are presented in Figure 5.

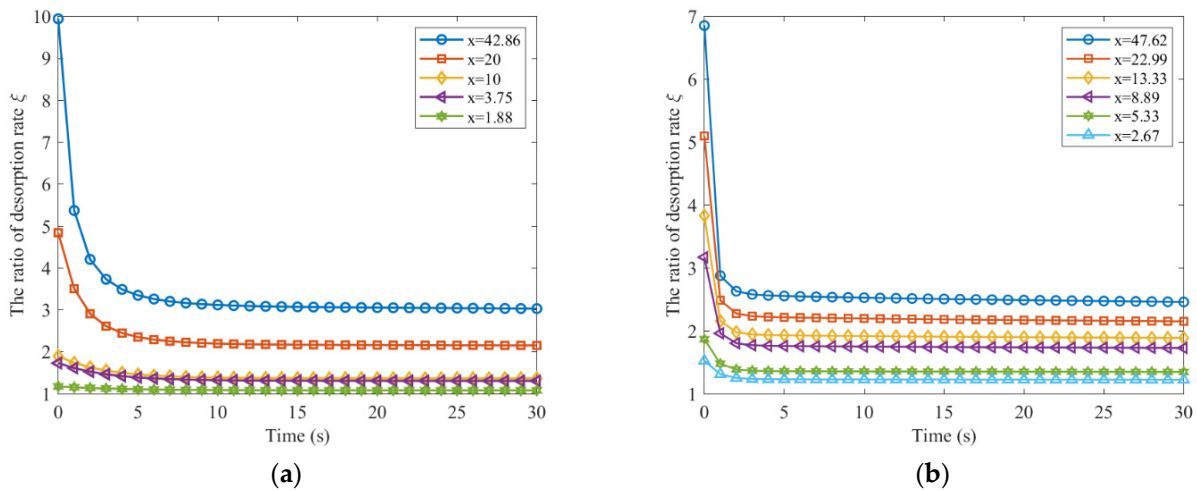


Figure 5. The ratio of gas desorption rate after and before coal is broken in a short time: (a) Effective diffusion coefficient from Yang; (b) Effective diffusion coefficient from Guo.

The ratio of gas desorption rate in coal before and after fragmentation decreases rapidly from a maximum value over a short period of time. The initial gas desorption rate ratio before and after coal crushing is greater for finer coal particles. The gas desorption rate decreases more quickly as the coal is further fragmented.

The ratio of the gas desorption rate in coal before and after fragmentation decreases slowly over time and approaches 0. The rate of decrease in the desorption rate ratio is faster for smaller particles, eventually reaching 0. The variation of gas desorption rate ratios during long-term desorption for coal particles of different crushing sizes is shown in Figure 6.

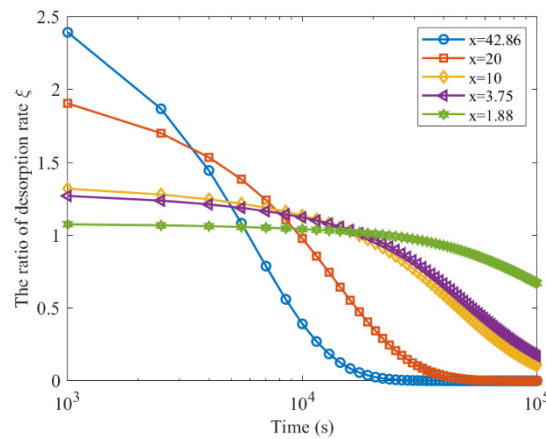


Figure 6. The ratio of gas desorption rate after and before coal is broken for a long time (Yang).

4.3. Relationship between Desorption Rate Ratio and Coal Particle Breakage Ratio

When $D_e t$ is small, meaning the effective diffusion coefficient is a constant, and time is not long, Equation (11) can be reduced to:

$$g(D_e t) = \frac{M_t}{M_\infty} = 6 \cdot \sqrt{\frac{D_e t}{\pi}} \tag{28}$$

In the initial time period, combining Equation (28) and Equation (16) can be reduced to:

$$\eta(t) = \sqrt{\frac{D_e(R_2)}{D_e(R_1)}} \tag{29}$$

In combination with Equations (20) and (29), the ratio of gas amount diffusing from coal before being broken to that from crushed coal during a time period t could be expressed by the ratio of coal particle size before and after coal breakage as:

$$\eta(t) = \left(\frac{R_1}{R_2}\right)^{\gamma/2} = x^{\gamma/2} \tag{30}$$

Equations (16) and (29) can be used to calculate the maximum and initial approximate ratio of accumulative gas desorption for coal particles of varying sizes relative to an initial diameter of 7.5 mm in Yang and 2 mm in Guo. The ratio of the initial period of cumulative desorption is approximately equal to the ratio of the maximum cumulative gas desorption.

In the initial period, the differential of the diffusivity is:

$$g'(D_e, t) = 3 \cdot \sqrt{\frac{D_e}{\pi t}} \tag{31}$$

The desorption rate ratio for the initial period is easily obtained as follows:

$$\zeta(t) = \sqrt{\frac{D_e(R_2)}{D_e(R_1)}} \tag{32}$$

Equations (29) and (32) demonstrate that the ratio of gas desorption volume from fragmented coal to that from intact coal equals the ratio of gas desorption rate during a given time period. Both ratios can be estimated by taking the square root of the ratio of the effective gas diffusion coefficient for broken coal particles to that for original coal particles.

By combining Equations (20) and (32), the ratio of the gas desorption rate in crushed coal to that in undisturbed coal during a specific time period can be expressed as the ratio of the coal particle size before and after fragmentation:

$$\zeta(t) = \left(\frac{R_1}{R_2}\right)^{\gamma/2} = x^{\gamma/2} \tag{33}$$

Equation (33) demonstrates that the ratio of desorption amount is equivalent to the ratio of gas desorption rate during the initial period.

The Equation (33) was used to fit the relationship between the coal particle breakage ratio and the gas desorption rate ratio after and before coal fragmentation. The results are depicted in Figure 7.

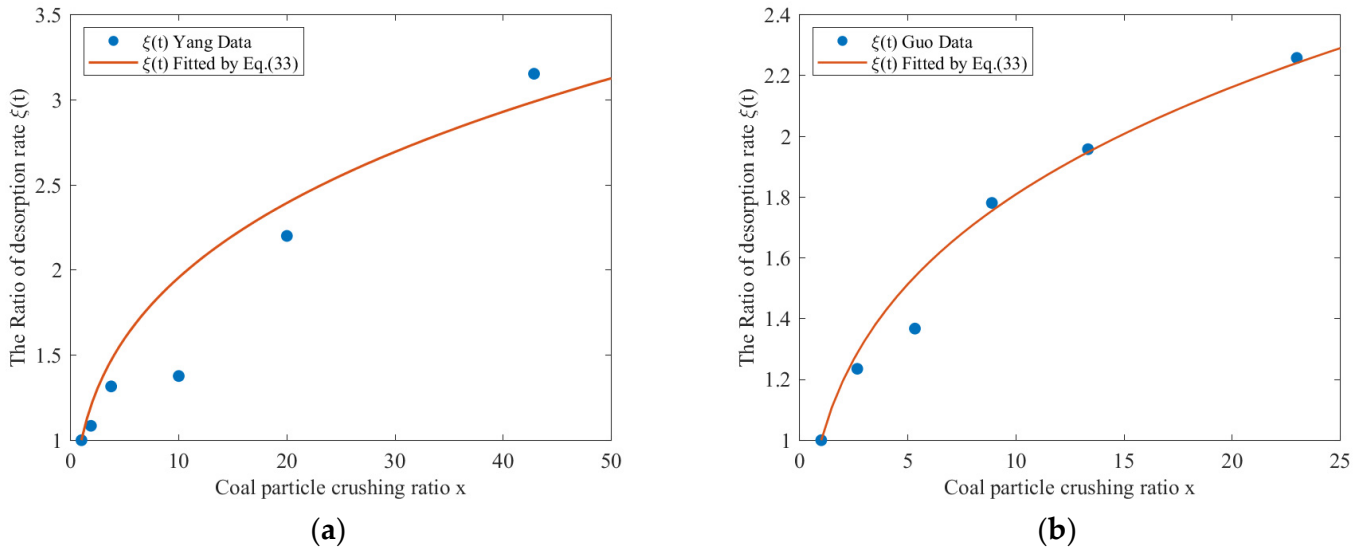


Figure 7. Relationship between the gas desorption rate ratio and the coal particle breakage ratio (a) Effective diffusion coefficient from Yang; (b) Effective diffusion coefficient from Guo.

The data fit parameters γ for Yang and Guo were 0.5829 and 0.5149, respectively, with coefficients of determination of 0.9303 and 0.9822, respectively. Figure 7 illustrates the approximate value for the ratio of the gas desorption rate from broken coal to that from intact coal after desorption lasts for a time period t .

The ratio of the gas diffusing rate from broken coal particles at the initial time to that from intact coal can be related to the coal particle breakage ratio $x = R_2/R_1$ from Equation (18):

$$\zeta(0) = x^\gamma \tag{34}$$

This $\zeta(0)$ is the initial value for the ratio of the gas release rate from broken coal to that from coal before being broken, which is the largest value for the ratio. The initial gas desorption rate ratio is proportional to the coal particle breakage ratio.

4.4. Calculate the Desorption Rate Ratio with Particle Distribution

Assuming that prior to the occurrence of coal and gas outbursts, the coal was composed of centimeter-sized coal particles, under the influence of factors such as geological stress, coal and gas outbursts occurred, causing the coal to break into particles of different sizes. Additionally, the coal particles are also broken due to collisions with each other during the outburst. For instance, the coal sample with a particle size of 1–2 mm and a mass of 50 g was ground and crushed using a ball mill at 150 r/min and 250 r/min [53]. The mass of the coal sample after sieving can be seen in Table 2.

Table 2. The mass of the coal particles after sieving at different speeds.

Diameter/mm	Mass/g	
	Cai-1 (150 r/min)	Cai-2 (250 r/min)
0–0.075	0	8.8763
0.075–0.125	0.0152	5.5584
0.125–0.18	0.04256	6.9523
0.18–0.425	0.8574	12.0993
0.425–1	2.8517	14.8428
1–2	44.4852	0.8513

After outbursts occurred in the Zhongliangshan Coal Mine, the outburst coal samples were sieved. The sieving results of coal samples after two outbursts are provided in Table 3 [54].

Table 3. Sieving results of coal samples in outburst coal seams.

Diameter/mm	Proportion/%	
	Zhong-1	Zhong-2
<0.1	4.3	6.6
0.1–1	29.9	27.5
1–5	21.6	16.9
5–10	14.1	18.2
>10	27.1	30.8

The coal particles were ground and crushed using a ball mill, and the crushed coal was then sieved for particle size analysis. The mass distribution of the sieved particles was fitted using Equation (22), and the fitting results are depicted in Figure 8. The fitting parameters are recorded in Table 4.

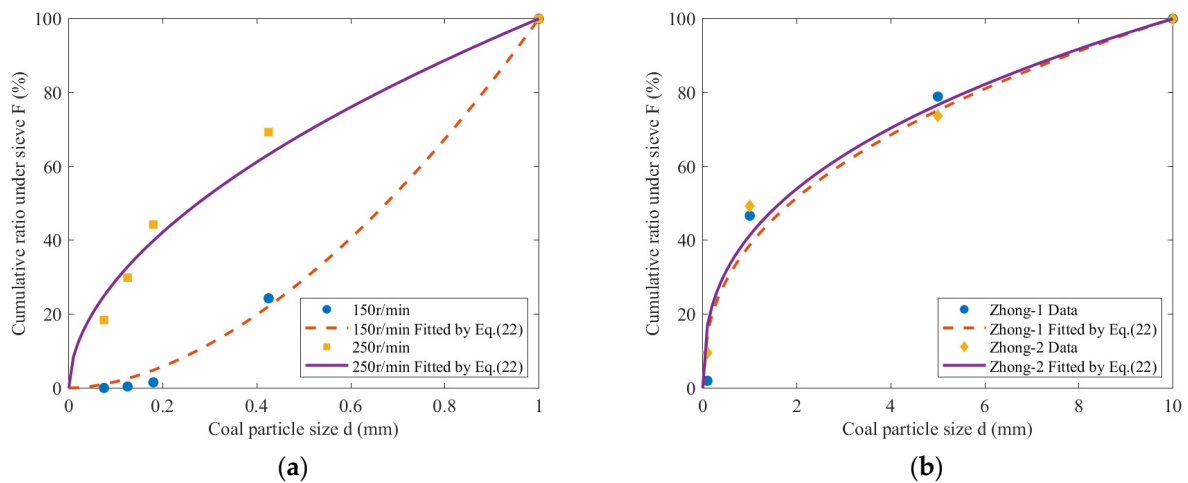


Figure 8. Cumulative ratio under sieve. (a) Data from Cai; (b) Data from Hu.

Table 4. Parameters of coal crushing.

No.	Distribution Index of Granularity α	Coefficient of Determination
Cai-1	1.7647	0.9980
Cai-2	0.5359	0.9788
Zhong-1	0.4121	0.9644
Zhong-2	0.3834	0.9722

Figure 8 reveals that the particle size distribution after coal crushing conforms to the GGS model. The finer the coal was broken, the smaller the distribution index of granularity α .

By substituting the data from Tables 1 and 4 into Equation (27), the desorption rate ratio before and after crushing were calculated. The relationship between the desorption rate ratio and the distribution index of granularity α is shown in Figure 9.

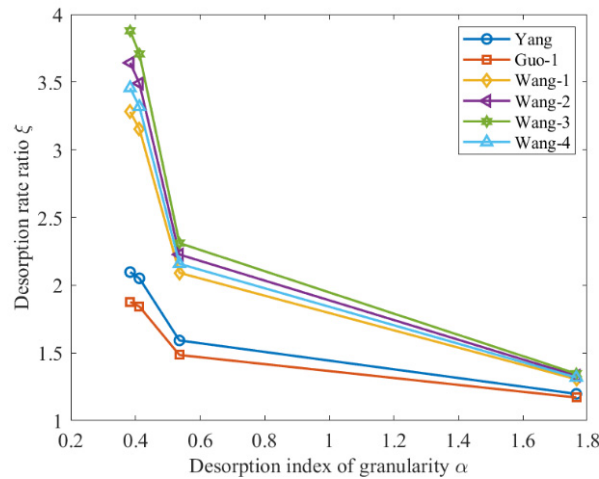


Figure 9. Relationship between desorption rate ratio and distribution index of granularity.

Figure 9 indicates that the desorption rate ratio increases with a decrease in the distribution index of granularity α when the index of desorption γ is constant. With the increase in the index of desorption γ , the ratio of desorption rate after and before coal crushing increases.

5. Discussion

The coal samples were collected from coal seam No. 5 in the Panzhihua coal mine located in western Guizhou, China. The moisture, ash, and volatile matter of coal were determined according to GB/T 212-2008. Referring to GB/T 217-2008 and GB/T 23561-2009, the apparent density ρ and porosity φ of coal were determined. The adsorption constants a and b of coal were determined by the high-pressure volumetric method. The results are shown in Table 5.

Table 5. Basic parameters of coal sample.

Analysis of Coal Industry				$\rho/(g/cm^{-3})$	$\varphi/\%$	$a/(cm^3/g)$	$b/(1/MPa)$
Mad/%	Aad/%	Vad/%	Fcad/%				
1.1	15	17.28	66.62	1.425	5	30	1

The cumulative gas desorption amount in unit mass coal Q_t is mainly determined by the total amount of gas adsorbed by coal in an adsorption equilibrium state and the effective diffusion coefficient of coal. The limit of diffusion is the difference between the initial gas content Q_a and the final gas content Q_{a0} at the same temperature and atmospheric pressure. It is $Q_\infty = Q_a - Q_{a0}$. The gas content under experimental conditions is calculated according to the following Equation (35).

$$\begin{aligned}
 Q &= Q_a + Q_f \\
 Q_a &= \frac{abp}{1 + bp} \cdot \frac{100 - A_d - W}{100} \cdot \frac{1}{1 + 0.31W} \\
 Q_f &= \frac{10p\phi \cdot 273}{\rho(273 + t_w)}
 \end{aligned}
 \tag{35}$$

where Q is the total gas content, cm^3/g , a and b are adsorption constant of combustible base, p is adsorption equilibrium pressure, MPa, A_d is ash on a dry basis, W is water content. ρ is apparent density of coal, g/cm^3 , ϕ is porosity. t_w is equilibrium temperature, $^\circ\text{C}$.

When the adsorption equilibrium pressure is constant, the diffusion capacity of methane in coal can be characterized by the diffusivity at different times. The diffusivity is the ratio of the cumulative desorption amount to the limit desorption amount. It is:

$$\frac{Q_t}{Q_\infty} = \frac{M_t}{M_\infty} \tag{36}$$

where Q_t is cumulative gas desorption amount in unit mass coal; Q_∞ is limit gas desorption amount in unit mass coal.

The amount of free gas released in a short period is:

$$Q_{ft} = \frac{10p\phi \cdot 273}{\rho(273 + t_w)} - \frac{\phi \cdot 273}{\rho(273 + t_w)} \tag{37}$$

The amount of adsorption gas released in a short period is (for convenience of comparison, the time is set to 30 s).

$$Q_{at} = g(D_e(R), t) \cdot \left(\frac{abp}{1 + bp} - \frac{ab}{10 + b} \right) \cdot \left(\frac{100 - A_d - W}{100} \frac{1}{1 + 0.31W} \right) \tag{38}$$

Put the values in Table 5 into Equations (37) and (38), and the amount of free gas and adsorbed gas released when the coal is broken into coal of different particle sizes after 30 s is calculated. The amount of gas released by coal with different particle sizes at different adsorption equilibrium pressures is shown in Figure 10.

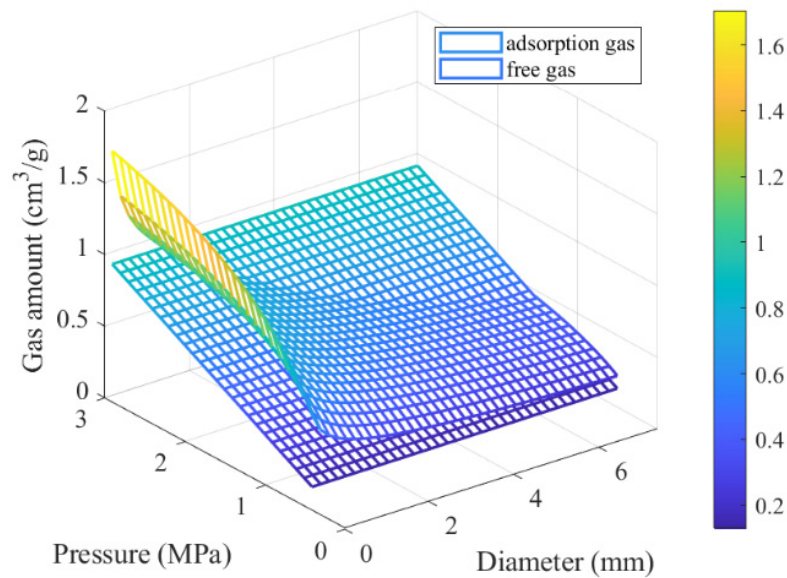


Figure 10. The amount of gas released by coal with different particle sizes at different adsorption equilibrium pressures.

When the adsorption equilibrium pressure remains constant, such as at 1 MPa, the adsorption and free gas released amounts vary with particle size and time, as illustrated in Figure 11.

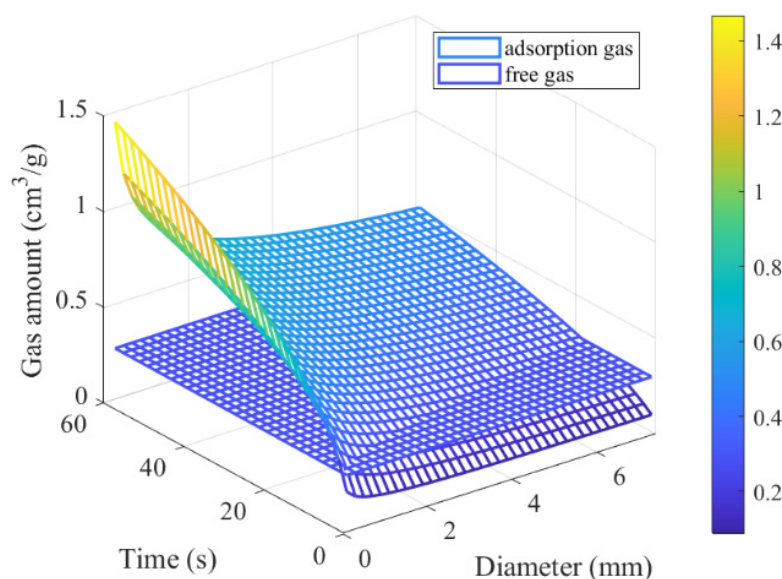


Figure 11. The amount of gas released by coal with different particle sizes at different times.

Figures 10 and 11 illustrate that the desorption amount of adsorbed gas increases as the particle size decreases at a given adsorption equilibrium pressure.

For coal in this study collected from Yangquan coal mine in Shanxi province, North China, when the coal is broken from the size range of 5–10 mm to the size less than 0.075 mm, the size ratio for coal particles before and after being broken is up to 100.

Both the corresponding cumulative gas desorption and desorption rates from broken coal are 4.6 times larger than those from intact coal within the same short time period, and the gas desorption rate from broken coal approximately increases by 21.5 times compared with the gas release rate from coal before being broken at the initial time. At an adsorption equilibrium pressure of 1 MPa, the free gas is $0.3161 \text{ cm}^3/\text{g}$, and the adsorption gas content is $13.3367 \text{ cm}^3/\text{g}$. Within 30 s, when the coal mass is crushed to 7.5 mm, the released free gas volume is $0.2845 \text{ cm}^3/\text{g}$, and the released adsorption gas volume is $1.0585 \text{ cm}^3/\text{g}$. Further crushing the coal to 0.075 mm, the released adsorption gas volume is $3.7445 \text{ cm}^3/\text{g}$. Therefore, when an outburst occurs, coal will be broken by the combined ground stress and drag force caused by flowing gas through coal. Broken coal would release a large amount of gas in a short time to further aggravate or sustain the outburst, which might explain how adsorbed gas within coal takes part in the coal and gas outburst. The accuracy of the desorption model for broken coal depends on the diffusion model and particle size distribution of the coal particles. In these diffusion models, coal particles are typically assumed to be spherical. The effective diffusion coefficient decreases as diffusion time increases. At the same time, in a short time period like 30 s, the effective diffusion coefficient changes little, and the outburst is short-lived. Therefore, when estimating the amount of desorbed gas during an outburst, it is assumed that the effective diffusion coefficient remains constant. Theoretical analysis provides an explanation for the correlation between smaller broken coal sizes and faster gas release rates, shedding light on the mechanism behind the sudden and massive gas emissions during coal and gas outbursts.

6. Conclusions

This study analyzed the changes in gas release rate and cumulative gas released from broken coal through the use of a broken coal gas desorption model. The conclusions of this study are summarized as follows:

- (1) A gas desorption model for broken coal was developed to elucidate the desorption behavior of coal mixtures containing particles of different sizes. The model incorpo-

rates the diffusivity of coal particles with varying sizes and the distribution function of coal particles.

- (2) The concept of gas desorption rate ratio was introduced to characterize the changes in the gas desorption rate of coal before and after crushing. The desorption rate ratio is mainly determined by the desorption index γ and the granularity distribution index α .
- (3) Within the limit range of coal particle sizes, the ratio of effective diffusion coefficient for coal particles with different sizes is directly proportional to the reciprocal of the ratio of particle sizes. When coal is of a single particle size before and after crushing, the gas desorption rate ratio of gas-bearing coal is the square root of the reciprocal of the effective diffusion coefficient.

Author Contributions: Conceptualization, Q.C. and G.H.; Data curation, Q.C., Z.L. and J.Z.; Formal analysis, Q.C. and Z.L.; Funding acquisition, G.H.; Investigation, Q.C. and Q.L.; Methodology, Q.C., G.H. and Z.L.; Resources, Z.L.; Software, J.Z.; Supervision, G.H.; Visualization, J.Z. and Q.L.; Writing—original draft, Q.C. and J.Z.; Writing—review and editing, J.Z. and Q.L. All authors have read and agreed to the published version of the manuscript.

Funding: This research was funded by the National Natural Science Foundation of China, grant number 51674049.

Institutional Review Board Statement: Not applicable.

Informed Consent Statement: Not applicable.

Data Availability Statement: Data are available at qiangcheng@cqu.edu.cn.

Conflicts of Interest: The authors declare that they have no known competing financial interests or personal relationships that could have appeared to influence the work reported in this paper.

References

1. Black, D.J. Review of coal and gas outburst in Australian underground coal mines. *Int. J. Min. Sci. Technol.* **2019**, *29*, 815–824. [[CrossRef](#)]
2. Fisne, A.; Esen, O. Coal and gas outburst hazard in Zonguldak Coal Basin of Turkey, and association with geological parameters. *Nat. Hazards* **2014**, *74*, 1363–1390. [[CrossRef](#)]
3. Shepherd, J.; Rixon, L.K.; Griffiths, L. Outbursts and geological structures in coal mines: A review. *Int. J. Rock Mech. Min. Sci. Geomech. Abstr.* **1981**, *18*, 267–283. [[CrossRef](#)]
4. Chen, K.P. A new mechanistic model for prediction of instantaneous coal outbursts—Dedicated to the memory of Prof. Daniel D. Joseph. *Int. J. Coal Geol.* **2011**, *87*, 72–79. [[CrossRef](#)]
5. Beamish, B.B.; Crosdale, P.J. Instantaneous outbursts in underground coal mines: An overview and association with coal type. *Int. J. Coal Geol.* **1998**, *35*, 27–55. [[CrossRef](#)]
6. Fan, C.; Li, S.; Luo, M.; Du, W.; Yang, Z. Coal and gas outburst dynamic system. *Int. J. Min. Sci. Technol.* **2017**, *27*, 49–55. [[CrossRef](#)]
7. Zhai, C.; Xiang, X.; Xu, J.; Wu, S. The characteristics and main influencing factors affecting coal and gas outbursts in Chinese Pingdingshan mining region. *Nat. Hazards* **2016**, *82*, 507–530. [[CrossRef](#)]
8. Liu, T.; Li, M.Y.; Zou, Q.L.; Li, J.F.; Lin, M.H.; Lin, B.Q. Crack instability in deep coal seam induced by the coupling of mining unloading and gas driving and transformation of failure mode. *Int. J. Rock Mech. Min. Sci.* **2023**, *170*, 105526. [[CrossRef](#)]
9. Sun, W.; Wang, N.; Chu, W.; Jiang, C. The role of volatiles and coal structural variation in coal methane adsorption. *Sci. Bull.* **2015**, *60*, 532–540. [[CrossRef](#)]
10. Liu, P.; Qin, Y.; Liu, S.; Hao, Y. Numerical Modeling of Gas Flow in Coal Using a Modified Dual-Porosity Model: A Multi-Mechanistic Approach and Finite Difference Method. *Rock Mech. Rock Eng.* **2018**, *51*, 2863–2880. [[CrossRef](#)]
11. Xu, H.; Qin, Y.; Wu, F.; Zhang, F.; Liu, W.; Liu, J.; Guo, M. Numerical modeling of gas extraction from coal seam combined with a dual-porosity model: Finite difference solution and multi-factor analysis. *Fuel* **2022**, *313*, 122687. [[CrossRef](#)]
12. Sun, L.; Wang, H.; Zhang, C.; Zhang, S.; Liu, N.; He, Z. Evolution of methane ad-/desorption and diffusion in coal under the presence of oxygen and nitrogen after heat treatment. *J. Nat. Gas Sci. Eng.* **2021**, *95*, 104196. [[CrossRef](#)]
13. Busch, A.; Gensterblum, Y. CBM and CO₂-ECBM related sorption processes in coal: A review. *Int. J. Coal Geol.* **2011**, *87*, 49–71. [[CrossRef](#)]
14. Zang, J.; Wang, K. A numerical model for simulating single-phase gas flow in anisotropic coal. *J. Nat. Gas Sci. Eng.* **2016**, *28*, 153–172. [[CrossRef](#)]
15. Airey, E.M. Gas emission from broken coal. an experimental and theoretical investigation. *Int. J. Rock Mech. Min. Sci.* **1968**, *5*, 475–494. [[CrossRef](#)]

16. Cheng, Y.; Pan, Z. Reservoir properties of Chinese tectonic coal: A review. *Fuel* **2020**, *260*, 116350. [[CrossRef](#)]
17. Tu, Q.; Cheng, Y.; Xue, S.; Ren, T. Effect of particle size on gas energy release for tectonic coal during outburst process. *Fuel* **2022**, *307*, 121888. [[CrossRef](#)]
18. Zhou, A.; Zhang, M.; Wang, K.; Elsworth, D.; Deng, N.; Hu, J. Rapid gas desorption and its impact on gas-coal outbursts as two-phase flows. *Process Saf. Environ. Protect.* **2021**, *150*, 478–488. [[CrossRef](#)]
19. Zhang, M.; Cao, X.; Li, B.; Zhou, A. Quantitative study on the role of desorption gas on coal-gas outbursts: Energy contribution and dynamic characteristics. *Process Saf. Environ. Protect.* **2023**, *171*, 437–446. [[CrossRef](#)]
20. Jin, K.; Cheng, Y.; Ren, T.; Zhao, W.; Tu, Q.; Dong, J.; Wang, Z.; Hu, B. Experimental investigation on the formation and transport mechanism of outburst coal-gas flow: Implications for the role of gas desorption in the development stage of outburst. *Int. J. Coal Geol.* **2018**, *194*, 45–58. [[CrossRef](#)]
21. Wang, S.; Elsworth, D.; Liu, J. Mechanical Behavior of Methane Infiltrated Coal: The Roles of Gas Desorption, Stress Level and Loading Rate. *Rock Mech. Rock Eng.* **2013**, *46*, 945–958. [[CrossRef](#)]
22. Yang, D.; Chen, Y.; Tang, J.; Li, X.; Jiang, C.; Wang, C.; Zhang, C. Experimental research into the relationship between initial gas release and coal-gas outbursts. *J. Nat. Gas Sci. Eng.* **2018**, *50*, 157–165. [[CrossRef](#)]
23. Lu, S.; Li, M.; Sa, Z.; Liu, J.; Wang, S.; Qu, M. Discrimination of gas diffusion state in intact coal and tectonic coal: Model and experiment. *Fuel* **2022**, *325*, 124916. [[CrossRef](#)]
24. Ye, Q.; Li, C.; Yang, T.; Wang, Y.; Li, Z.; Yin, Y. Relationship between desorption amount and temperature variation in the process of coal gas desorption. *Fuel* **2023**, *332*, 126146. [[CrossRef](#)]
25. Bertard, C.; Bruyet, B.; Gunther, J. Determination of desorbable gas concentration of coal (direct method). *Int. J. Rock Mech. Min. Sci. Geomech. Abstr.* **1970**, *7*, 43–65. [[CrossRef](#)]
26. Yang, Q.; Wang, Y. Theory of methane diffusion from coal cuttings and its application. *J. China Coal Soc.* **1986**, *3*, 87–94.
27. Busch, A.; Gensterblum, Y.; Krooss, B.M.; Littke, R. Methane and carbon dioxide adsorption–diffusion experiments on coal: Upscaling and modeling. *Int. J. Coal Geol.* **2004**, *60*, 151–168. [[CrossRef](#)]
28. Yao, Y.; Qin, Y.; Yu, H. Study on gas adsorption and desorption in coal sample. *J. Liaoning Tech. Univ. (Nat. Sci.)* **2009**, *28*, 701–703.
29. Barrer, R.M. *Diffusion in and through Solids*; The Syndics of the Cambridge University Press: Cambridge, UK, 1951.
30. Nandi, S.P.; Walker, P.L. Activated diffusion of methane in coal. *Fuel* **1970**, *49*, 309–323. [[CrossRef](#)]
31. Crank, J. *The Mathematics of Diffusion*–Oxford University Press, 2nd ed.; Oxford University Press: Oxford, UK, 1975.
32. Smith, D.M.; Williams, F.L. Diffusion models for gas production from coals: Application to methane content determination. *Fuel* **1984**, *63*, 251–255. [[CrossRef](#)]
33. Ruckenstein, E.; Vaidyanathan, A.S.; Youngquist, G.R. Sorption by solids with bidisperse pore structures. *Chem. Eng. Sci.* **1971**, *26*, 1305–1318. [[CrossRef](#)]
34. Clarkson, C.R.; Bustin, R.M. The effect of pore structure and gas pressure upon the transport properties of coal: A laboratory and modeling study. 2. Adsorption rate modeling. *Fuel* **1999**, *78*, 1345–1362. [[CrossRef](#)]
35. Shi, J.Q.; Durucan, S. A bidisperse pore diffusion model for methane displacement desorption in coal by CO₂ injection. *Fuel* **2003**, *82*, 1219–1229. [[CrossRef](#)]
36. Li, Z.; Liu, D.; Cai, Y.; Shi, Y. Investigation of methane diffusion in low-rank coals by a multiporous diffusion model. *J. Nat. Gas Sci. Eng.* **2016**, *33*, 97–107. [[CrossRef](#)]
37. Li, Z.; Liu, Y.; Xu, Y.; Song, D. Gas diffusion mechanism in multi-scale pores of coal particles and new diffusion model of dynamic diffusion coefficient. *J. China Coal Soc.* **2016**, *41*, 633–643.
38. Li, Z.; Wang, D.; Song, D. Influence of temperature on dynamic diffusion coefficient of CH₄ into coal particles by new diffusion model. *J. China Coal Soc.* **2015**, *40*, 1055–1064.
39. Li, Z.; Peng, J.; Li, L.; Qi, L.; Li, W. Novel Dynamic Multiscale Model of Apparent Diffusion Permeability of Methane through Low-Permeability Coal Seams. *Energy Fuels* **2021**, *35*, 7844–7857. [[CrossRef](#)]
40. Li, Z.; Li, L.; Peng, J.; Karrech, A.; Liu, Y. Model and Experiment of Multiscale Dynamic Permeability in Series for Coalbed Gas Flowing through Micro–Nanopores. *Energy Fuels* **2022**, *36*, 10845–10859. [[CrossRef](#)]
41. Li, Z.; Chen, J.; Li, L.; Peng, J. Experiment, modelling, mechanism and significance of multiscale and dynamic diffusion-permeability of gas through micro-nano series pores in coal. *J. China Coal Soc.* **2023**, *48*, 1551–1566.
42. Zhao, W.; Cheng, Y.; Pan, Z.; Wang, K.; Liu, S. Gas diffusion in coal particles: A review of mathematical models and their applications. *Fuel* **2019**, *252*, 77–100. [[CrossRef](#)]
43. Guo, H.; Cheng, Y.; Ren, T.; Wang, L.; Yuan, L.; Jiang, H.; Liu, H. Pulverization characteristics of coal from a strong outburst-prone coal seam and their impact on gas desorption and diffusion properties. *J. Nat. Gas Sci. Eng.* **2016**, *33*, 867–878. [[CrossRef](#)]
44. Zheng, J.; Liang, Q.; Zhang, X.; Huang, J.; Yan, W.; Huang, G.; Liu, H. On Gas Desorption-Diffusion Regularity of Bituminous Coal with Different Particle Sizes and Its Influence on Outburst-Coal Breaking. *Sustainability* **2023**, *15*, 9894. [[CrossRef](#)]
45. Zhao, W.; Cheng, Y.; Jiang, H.; Jin, K.; Wang, H.; Wang, L. Role of the rapid gas desorption of coal powders in the development stage of outbursts. *J. Nat. Gas Sci. Eng.* **2016**, *28*, 491–501. [[CrossRef](#)]
46. Irani; Riyad, R. *Particle Size: Measurement, Interpretation, and Application*; John Wiley & Sons, Inc.: New York, NY, USA; London, UK, 1963.
47. Wang, L.; Wang, H.; Zhu, J.; Huang, W.; Zhao, Y. Experimental study on particle size distribution of impact crushed coal containing gas. *Fuel* **2022**, *325*, 124745. [[CrossRef](#)]

48. Hou, S.H.; Wang, X.M.; Wang, X.J.; Yuan, Y.D.; Pan, S.D.; Wang, X.M. Pore structure characterization of low volatile bituminous coals with different particle size and tectonic deformation using low pressure gas adsorption. *Int. J. Coal Geol.* **2017**, *183*, 1–13. [[CrossRef](#)]
49. Zhang, X.; Sang, S.; Qin, Y.; Zhang, J.; Tang, J. Isotherm adsorption of coal samples with different grain size. *J. China Univ. Min. Technol.* **2005**, *34*, 427–432.
50. Liu, Y.; Liu, M. Effect of particle size on difference of gas desorption and diffusion between soft coal and hard coal. *J. China Coal Soc.* **2015**, *40*, 579–587.
51. Cheng, X.; Wang, Z.; Li, Z. Features of gas diffusion in tectonic coal with different particle sizes by new model of dynamic diffusion coefficient. *J. Saf. Sci. Technol.* **2016**, *12*, 88–93.
52. Wang, Z. Research on Microstructure Evolution of Tectonic Coal and Its Influence on Gas Adsorption and Desorption Kinetics. Ph.D. Thesis, China University of Mining and Technology, Beijing, China, 2020.
53. Cai, Z.; Huang, G.; Zheng, J.; Cheng, Q.; Geng, W. Experimental study on the relationship between mode I static fracture toughness and newly added surface area after crushing. *Chin. J. Rock Mech. Eng.* **2021**, *40*, 1570–1579.
54. Hu, Q.; Wen, G. *Mechanical Mechanism of Coal and Gas Outburst*; Science Press: Beijing, China, 2013; pp. 67–68.

Disclaimer/Publisher’s Note: The statements, opinions and data contained in all publications are solely those of the individual author(s) and contributor(s) and not of MDPI and/or the editor(s). MDPI and/or the editor(s) disclaim responsibility for any injury to people or property resulting from any ideas, methods, instructions or products referred to in the content.